Microwave Review
December 2024, Vol. 30, No. 2, pp. 60-70
DOI: 10.18485/mtts_mr.2024.30.2.8

Comparative Analysis of OCGA-Based Sparse K/Ka Band Horn Antenna Structures at Different Frequencies

Manh Tuan Nguyen, Adnan F. Alhaj Hasan, Talgat R. Gazizov

Abstract – **Reducing the antenna mass while maintaining its desired characteristics is associated with many challenges. The optimal current grid approximation and its modified versions provide the possibility of creating sparse antennas with controllable characteristic accuracy while considerably minimizing their mass compared to their original structure. However, for antennas operating in wide frequency bands, it is necessary to consider that the current distribution through the wires of the original grid will change as the frequency changes. This leads to different sparse structures after applying these approaches. This paper investigates and compares the performance of sparse antenna structures obtained at different frequencies in the antenna operating frequency range. Different approximations are applied on a horn antenna designed to operate in the K/Ka band. Its sparse structures obtained at 18, 28 and 38 GHz were used for the analysis. Detailed analysis of the performance and advantages of the sparse antennas obtained after applying these approximations is performed. The analysis results allow the selection of a suitable sparse structure for specific applications. In addition, this paper also verifies the conclusions drawn in previous work for a different frequency band regarding at which frequency in the considered band the sparse structure must be generated.**

Keywords – **Wire-grid, sparse antennas, horn antennas, method of moments, optimal current grid approximation**

I. INTRODUCTION

With the rapid development of 5G and future 6G networks, the need for high-speed and stable data transmission is increasing [1–3]. To accommodate these demands, antennas must be able to operate over a wide frequency range, including the millimeter-wave range [4, 5]. They also must be capable of supporting multiple connected devices, from smartphones to Internet of Things (IoT) sensors, while at the same time operating on the principles of optimal frequency usage and minimal interference, especially in densely populated urban areas, to improve the user experience.

As the infrastructure of these networks is deployed in such areas, reducing the size and weight of antennas is becoming more and more important. This allows antennas to be integrated into advertising panels, street light poles, trees or even on the building's window glass without disrupting the aesthetics of the urban area [6, 7]. Additionally, this reduces the transportation and installation costs, which is especially important when it comes to both expanding the network coverage area and ensure the portability of the supported devices [8–10]. In general, reducing the antenna mass has a significant impact on reducing the overall manufacturing costs, and in some cases can improve the antenna performance [11, 12].

Article history: Received May 17, 2024; Accepted August 29, 2024

Manh Tuan Nguyen, Adnan F. Alhaj Hasan, Talgat R. Gazizov are with the Faculty of Radio Engineering, Tomsk State University of Control Systems and Radioelectronics, 40, prospect Lenina, 634050, Tomsk, Russian Federation, E-mail: nguyen.t.2213-2022@e.tusur.ru, alkhadzh@tusur.ru, talgat@tu.tusur.ru

On the other hand, mass reduction may affect the antenna performance and its important characteristics. Thus, there are challenges that must be considered and addressed to achieve the desired reduction [13, 14]. An effective way to minimize and predict the negative effects of weight reduction is to use computer modeling in antenna design and development. It has many valuable benefits, especially when considering aspects such as performance, durability and stability. Modeling allows one to evaluate antenna performance under different operating conditions, optimize antenna design, and predict its manufacturing costs before proceeding to the actual fabrication and deployment process [15, 16].

There are many different popular antenna modeling methods including method of moments (MoM), finite-difference time-domain method and finite element method. Each method has its own advantages and limitations. Depending on the specific requirements, a suitable method can be selected. Meanwhile, among these methods, using MoM for antenna modeling has many appreciable advantages, which make it popular in such research community [17–19]. One of these advantages is its ability to model antennas with diverse and complex structures, providing detailed and accurate information about their characteristics [20, 21]. Moreover, MoM has a simple algorithm, which makes it easier in implementation and faster in computation compared to other methods. On top of the above advantages, the most frequently used one is the ability of MoM to serve as a basis for developing new approaches to design novel antenna structures. Wire Grid (WG) is among some of these approaches that have a great potential for development. It is based on approximating the antenna conducting surface with a grid of wires [22, 23]. Researchers in [24, 25] used WG to reduce the antenna mass as well as the computational cost associated with its simulations. They also demonstrated that the use of WG allows to accurately determine the main antenna characteristics, which may help designers to analyze and optimize them with low computational cost.

Meanwhile, the development of sparse antennas has received much attention recently, considering the growing demands for reducing antenna mass and size [26, 27]. Moreover, the development of sparse WG antennas presents opportunities for their easy integration in compact devices such as IoT sensors and in areas such as vehicle on-glass antennas where space and mass are important constraints [28, 29].

Inheriting the advantages of MoM-based WG antennas, a new approach to design sparse antennas was proposed in [25]. This approach is known as optimal current grid approximation (OCGA). It provides an equivalent sparse antenna structure by eliminating wires with normalized current magnitudes below a given threshold comparing to the maximum or average current magnitude in the grid wires. This threshold is called the Grid Element Elimination Tolerance (GEET). OCGA has been applied on different antenna types [30]. However, its application on non-printed antenna designs faces several technical challenges due to the presence of wires unconnected to the main grid. To address this problem, a modified versions of the initial approximation were proposed in [31]. The first is referred to as the "eliminating" OCGA (EOCGA). In it, the connections between all remaining wires are checked and then the wires not connected to the main grid are eliminated. The second modification is called the "near-connecting" OCGA (NCOCGA). In it, only the necessary wires are recovered after OCGA to establish a connection between any free wire and the nearest one to it in the main grid.

In [32], a comprehensive comparative analysis of sparse structures derived only from the OCGA and connected OCGA (COCGA) approaches is performed for a wide-band perforated horn antenna. The successful approximation of the antenna surface is confirmed by comparison with HFSS simulation results and measurements of 3D-printed structures. The study showed that COCGA generally (with smaller GEET values) yields antenna characteristics closer to those for the original structure, indicating a higher accuracy in preserving the original characteristics, but OCGA surpasses COCGA in terms of mass reduction as well as time and memory requirements for further simulations. As is known and demonstrated in [32], the current distribution along the WG varies at different frequencies. This results in the appearance of different sparse structures after applying these approaches at diverged frequencies. The study recommended generating the sparse structure at the lowest frequency in the bandwidth since it can closely resemble the characteristics of the original antenna, and no matter at which frequency in the bandwidth the sparse antenna was obtained, the accuracy of the C/OCGA results increases with increasing the frequency. However, it was noted that manufacturers should choose the sparse structure with suitable GEET value based on their specific requirements as in some certain cases, structures derived at other frequencies provide superior results.

These findings emphasized the value of the analysis performed in [32] and the need for another one to evaluate the performance of sparse structures derived from the EOCGA and NCOCGA. Moreover, the analysis in [32] was conducted only for antennas operating in the X-band. Therefore, in order to generally understand the influence of the choice of the frequency at which the sparse structure can be generated on its characteristics, it is necessary to consider other frequency bands. Therefore, the main aim of this paper is to perform a comprehensive analysis and comparison of the performance of sparse antenna structures obtained after applying OCGA and all its modifications and operating in the K/Ka band 5G networks. The valuable contribution of this paper can help antenna designers and manufacturers to decide which approach is appropriate to choose for designing their sparse antenna as well as at which frequency it should be generated to obtain the desired characteristics.

This study is organized as follows. Section II presents the results of the surface approximation process of a K/Ka band horn antenna using WG. Then, it provides comparisons of the WG results obtained by different programs with each other and with simulation results of other methods as well as with measurements of the antenna model created using 3D printing technology. Section III presents the sparse antenna structures after applying OCGA and its modifications at the main (boundary and center) frequencies in the antenna operating frequency band. This section also provides a comparative analysis of each sparse structure performance, highlighting their similarities and differences. Furthermore, conclusions and recommendations made in earlier papers were verified add new ones were introduced. Section IV presents the sparse antennas obtained after applying different approaches with specific GEET values. A comprehensive analysis and comparison of the performance improvements achieved by these antennas over the entire operating frequency band are carried out. Section V summarizes the study findings and draws conclusions based on the conducted analysis.

II. Surface Approximation Using WG

To accomplish the purpose of this study, we chose a 3D-printed horn antenna made of conductive filament and described in [33]. This antenna is designed to operate in the K/Ka band for 5G networks. It consists of two parts: regular and irregular. The regular part of the antenna is a standard WR34 rectangular waveguide operating in the frequency range of 22–33 GHz. The waveguide geometrical parameters are: length a_1=8.35 mm, width b_1=3.85 mm and height l_1=4.32 mm. The irregular part of the horn antenna is an expanded extension of the waveguide that directs radio waves into beams. The geometric parameters of this part include the length a_2=22 mm, the width b_2=17.15 mm and the height l_2=13.25 mm. An isometric view of the antenna is shown in Fig. 1*a*.

First, the horn antenna is modeled using WG in [34]. The grid that approximates the antenna regular part was divided along the OX axis into 7 parts, OY axis – 6 parts and OZ axis – 10 parts. While the grid approximated the irregular part was divided along the OX axis into 7 parts, OY axis – 6 parts and along OZ axis –10 parts. A total of N=1139 wires was used to approximate the entire antenna surface. For the fabrication of the horn antenna prototype in [33], 0.4 mm thick Electrif material was used. Therefore, all grid wires had a radius r=0.2 mm. To excite the grid, a wire with a voltage difference of 1 V was connected to the grid on the underside of the regular part and inside it along the OY axis. This wire was placed in the center of the waveguide at a distance of $l_1/2$=2.16 mm from the closed waveguide surface. The excitation wire had a length of l_S=2.15 mm and radius of r_S=0.2 mm, and divided into 5 segments, while a single segment was used for the rest grid wires. Antenna structures approximated by WG in TALGAT and 4NEC2 systems are shown in Fig. 1*b*, *c*. To distinct these structures from the sparse ones in this study, they will be referred to hereafter as the original structures.

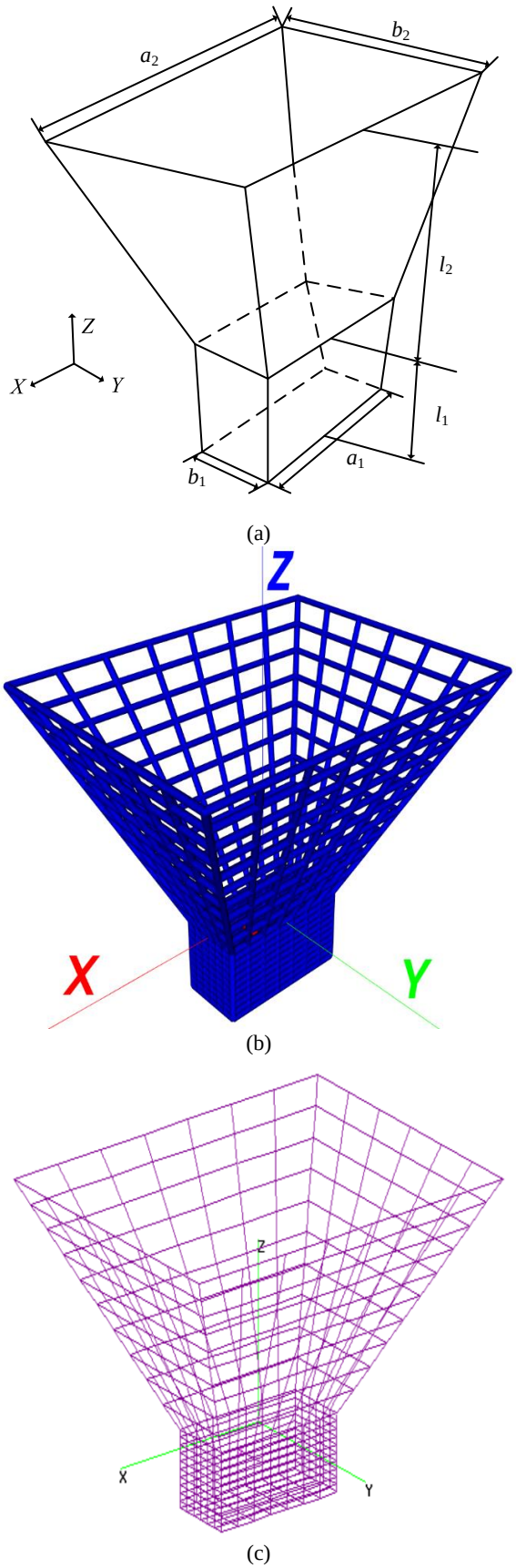

Fig. 1. (a) Isometric view of the 3D printed horn antenna, (b) its equivalent structures approximated by WG in TALGAT, and (c) 4NEC2 [34]

Next, the WG simulation results in TALGAT (with manual segmentation) and 4NEC2 (with manual and auto-segmentation) were compared with those obtained in [33] using the CST system for the same horn antenna model. These results were also compared with the measured ones for the 3D printed horn antenna made of conductive filament and described in [33]. The considered antenna characteristics of interest included the reflection coefficient magnitude ($|S_{11}|$) and the maximum gain (G_{max}) over the operating frequency range. A comparison of these characteristics was performed and presented here for further comparisons in Fig. 2. Besides that, to verify the directivity of the horn antenna, it is necessary to consider its radiation pattern (RP). The RPs obtained using WG in TALGAT were compared with those in CST, 4NEC2 (manual and auto-segmentation) and with the measured ones for the 3D-printed antenna with conductive filament Electrifi. The RPs were compared in the *E* and *H* planes, at the center frequency of 28 GHz and here presented for further comparisons in Fig. 3.

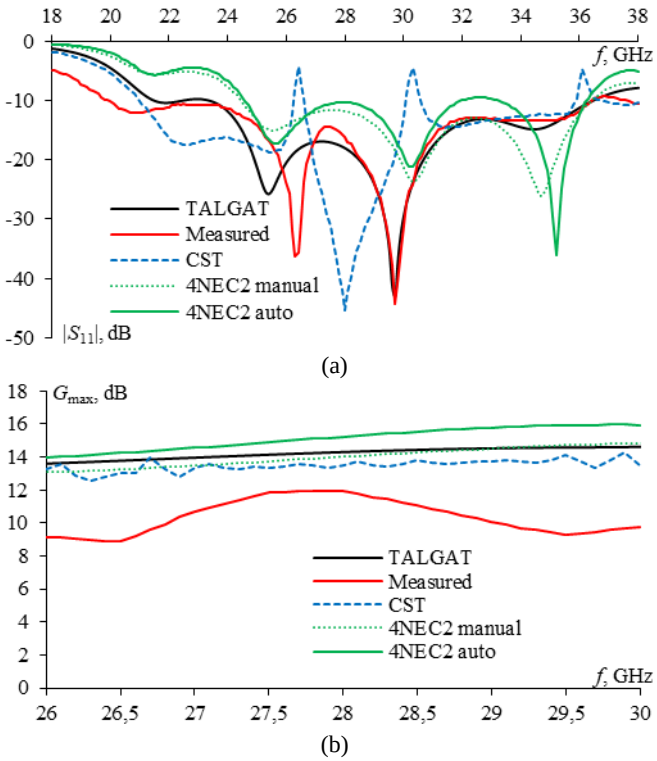

Fig. 2. Frequency dependences of the horn antenna obtained experimentally [33], numerically in CST [33], and numerically using WG in TALGAT and 4NEC2 (manual and auto-segmentation) [34]: (a) $|S_{11}|$, (b) G_{max}

The results in Fig. 2 and Fig. 3 are discussed in detail in [34]. Their comparative analysis data are summarized here in Table 1. The considered characteristics obtained for the horn antenna different models are the antenna bandwidth, resonant frequencies, and the G_{max}, the RP beam width (BW) and the side lobe level (SLL) at the central frequency. It was noticed that, in general, TALGAT gives results that are in better agreement with the measured ones compared to those obtained in CST and 4NEC2. The difference between the calculated and measured results might be attributed to the inevitable errors in the fabrication process using 3D printing technology.

TABLE 1
THE HORN ANTENNA CHARACTERISTICS OBTAINED FOR ITS DIFFERENT MODELS [34]

Antenna model	Bandwidth, GHz	Resonant frequencies, GHz	At a frequency of 28 GHz		
			G_{max}, dBi	SLL (*E*/*H*), dB	BW (*E*/*H*), °
Measured	16.5	29.7	12.0	22.37/17.69	38/31.5
CST	3.5	28	13.6	32.11/11.64	27/32
WG in TALGAT	14.8	29.7	14.3	23.24/18.24	34/32
WG in 4NEC2 manual segmentation	11.9	34.7	14.0	25.39/14.19	34/31
WG in 4NEC2 auto-segmentation	11.6	35.2	15.3	27.93/13.73	33/29

Meanwhile, in the *E* plane, the obtained simulation results in CST were slightly better than those in TALGAT and 4NEC2, e.g., lower SLL and BW, but they differed significantly with the measured ones. In the *H* plane, the obtained SLL in CST was higher than those in TALGAT and 4NEC2 and highly differed with measured one.

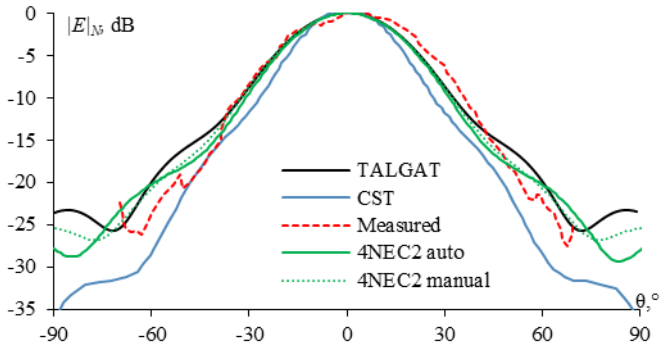

(a)

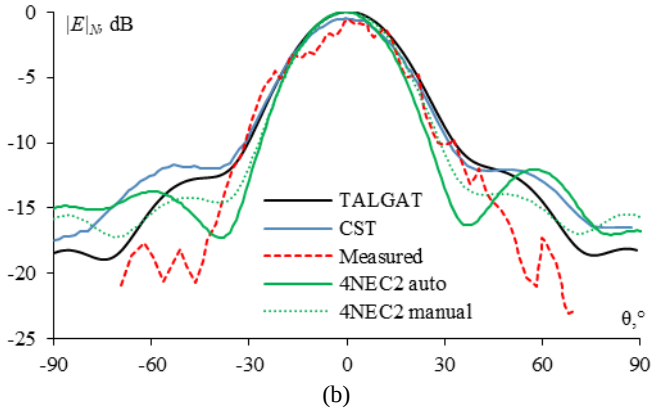

(b)

Fig. 3. Horn antenna RPs obtained at 28 GHz experimentally [33], numerically in CST [33], and numerically using WG in TALGAT and 4NEC2 (manual and auto-segmentation) [34] in: (a) *E*, (b) *H* planes

III. COMPARATIVE ANALYSIS OF SPARSE STRUCTURES

Based on what was done in [34] and briefly presented in section II, the effectiveness of the WG approach in approximating the surface of the horn antenna is demonstrated. Simulation results using WG in TALGAT were most similar to the measurement ones of the 3D-printed horn antenna prototype. Therefore, the TALGAT WG structure was selected to design sparse antennas by applying OCGA and its modifications on it. In the case of modeling a horn antenna using WG, the excitation wire is directly connected to grid, which results in much higher current along the wires near the connection point than others. To handle this issue, the current magnitudes along the grid wires (except their values along the excitation wire) were normalized relative to their average value.

The sparsity of the WG structures obtained after applying OCGA, EOCGA and NCOCGA mainly depends on the GEET value. By changing the GEET value, different numbers of wires are removed from the original WG. However, the current through the grid is distributed differently at each operating frequency. Therefore, different sparse structures can be obtained for the same GEET value. Although the differences in these structures may be quite small, they may have a noticeable impact on the antenna characteristics. Consequently, a comprehensive comparative analysis is necessary to evaluate the performance of the sparse antennas obtained at different frequencies (e.g., the main operating ones). The central frequency of 28 GHz and the boundary ones of 18 and 38 GHz are considered for comparison. To avoid confusion, the sparse structures obtained at these frequencies will be denoted as S_{28}, S_{18} and S_{38}, respectively.

First, the original WG is simulated at these frequencies and then the current distribution along its wires is calculated. Then, the current magnitudes are normalized with respect to their average value obtained at each frequency. After that, the OCGA, EOCGA and NCOCGA approaches with different GEET values are applied to obtain the sparse structures. By changing the GEET, the number of remaining wires in the grid is changed for each sparse structure. This is demonstrated in Fig. 4. The effect of GEET value after applying the considered approaches on reducing the antenna mass and the required memory and time for further simulations when using the sparse structures instead of the original one is investigated and the results are compared at different frequencies in Fig. 5.

From the data presented in Fig. 4 and Fig. 5, it can be drawn that for GEET<40%, the least number of remaining wires is observed for S_{18}, and for GEET>40% – for S_{38}. Consequently, when GEET<40%, the reduction of antenna mass and required memory and time for further simulations is best for S_{18} compared to S_{28} and S_{38}, and when GEET>40% – S_{38}, and the results of S_{18} and S_{28} are very similar.

GEET dependences after applying OCGA, EOCGA and NCOCGA for S_{18}, S_{28}, and S_{38} structures at 18, 28, and

38 GHz were calculated for the following antenna characteristics: G_{max}, voltage standing wave ratio (VSWR), $|S_{11}|$, and input impedance magnitude ($|Z|$). The obtained results are compared with those of the original structures (at GEET=0%, summarized in Table 2) and presented in Fig. 6–Fig. 9, respectively.

TABLE 2
ORIGINAL WG STRUCTURE ANTENNA CHARACTERISTICS AT THE MAIN FREQUENCIES

f, GHz	G_{max}, dBi	VSWR	$\|S_{11}\|$, dB	$\|Z\|$, Ohm
18	11.50	15.67	–1.11	55.91
28	14.30	1.29	–17.99	53.51
38	14.54	2.39	–7.75	115.90

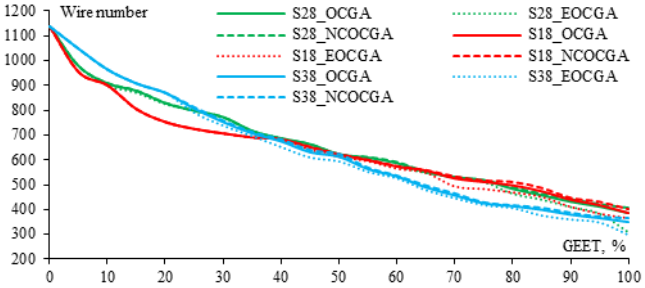

Fig. 4. GEET dependencies of the total number of remaining wires after OCGA, EOCGA and NCOCGA for S_{28}, S_{18} and S_{38}

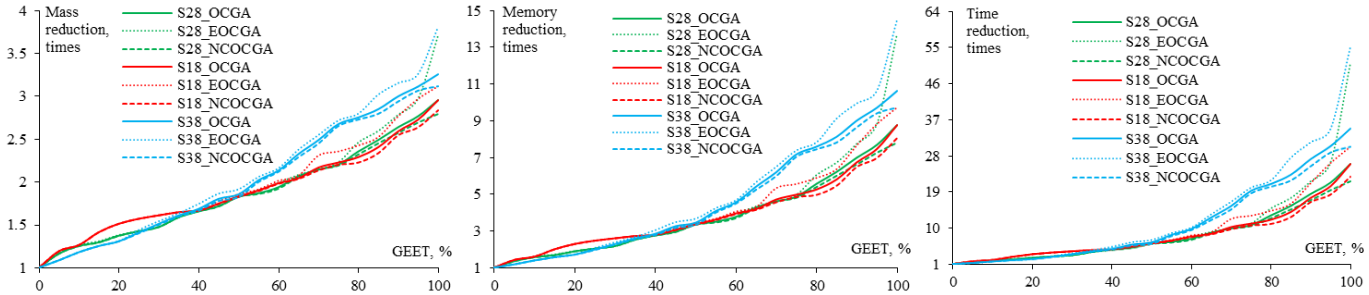

Fig. 5. GEET dependences of the reduction of the sparse WG horn antenna for further simulations after OCGA, EOCGA and NCOCGA for S_{28}, S_{18} and S_{38}: (a) mass, (b) required memory, and (c) time

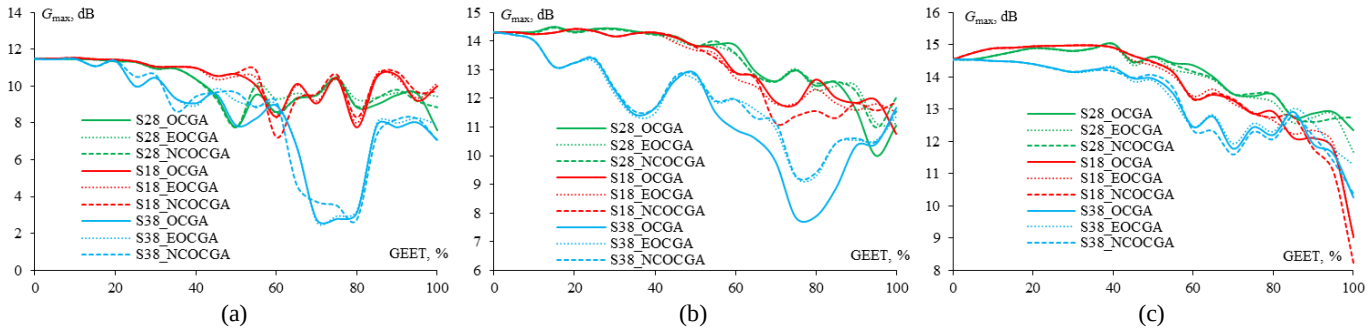

Fig. 6. GEET dependences of G_{max} after OCGA, EOCGA and NCOCGA for S_{18}, S_{28} and S_{38} at: (a) 18 GHz, (b) 28 GHz, (c) 38 GHz

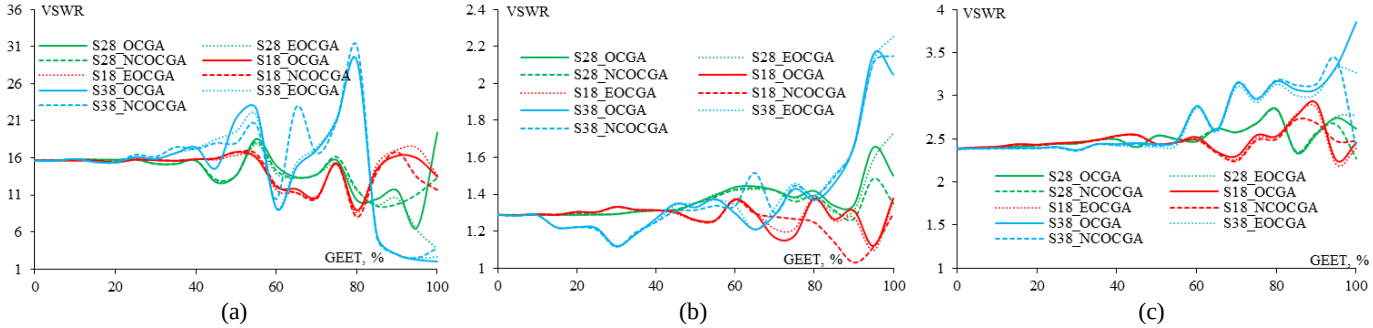

Fig. 7. GEET dependences of VSWR after OCGA, EOCGA and NCOCGA for S_{18}, S_{28} and S_{38} at: (a) 18 GHz, (b) 28 GHz, (c) 38 GHz

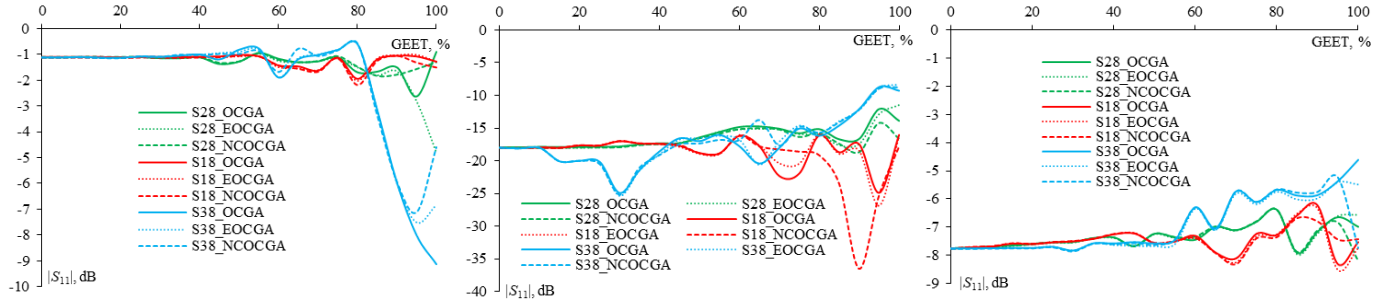

(a) (b) (c)

Fig. 8. GEET dependences of $|S_{11}|$ after OCGA, EOCGA and NCOCGA for S_{18}, S_{28} and S_{38} at: (a) 18 GHz, (b) 28 GHz, (c) 38 GHz

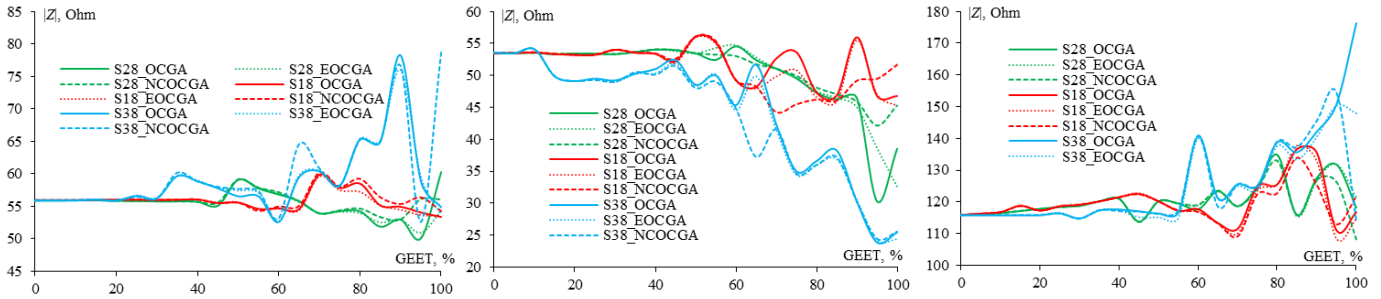

(a) (b) (c)

Fig. 9. GEET dependences of $|Z|$ after OCGA, EOCGA and NCOCGA for S_{18}, S_{28} and S_{38} at: (a) 18 GHz, (b) 28 GHz, (c) 38 GHz

When comparing all the antenna characteristics, it can be observed that when GEET<40%, the difference between the obtained results at 18 and 28 GHz for S_{18} and S_{28} is insignificant compared to the original WG. While the difference of the S_{38} results is insignificant only when GEET<20% at 18 GHz and when GEET<10% at 28 GHz. This difference is also insignificant at the frequency of 38 GHz for all structures when GEET<50%. This demonstrates that sparse structures obtained when GEET<50% at any frequency in the frequency range give best results when operate at high frequencies. This consists with the conclusions made in [32] for a different antenna operating at different frequency range after applying OCGA and COCGA.

In general, as the GEET value increases (especially when GEET>50%), the difference becomes more noticeable for all sparse structures. In particular, in Fig. 6, the G_{max} results show that S_{18} and S_{28} give similar results and better ones than those for S_{38}. This is also can be concluded for the VSWR results in Fig. 7, which also show that when GEET>50%, S_{18} has the lowest VSWR value compared to S_{28} and S_{38}. At the central frequency of 28 GHz and for all GEET values, the obtained VSWR values for all structures are always less than 2.2 and for S_{18} they are even always less than 1.4. The same conclusions as for VSWR and G_{max} can be drawn for $|S_{11}|$ and $|Z|$ results from Fig. 8 and Fig. 9. From the comparison results, it can be observed that in general, S_{18} has advantages over other structures since its characteristics vary less with changing the GEET value.

When comparing the results obtained for all structures, it can be observed that in general there is no significant difference between the results after applying OCGA, EOCGA and NCOCGA. The difference is only observed at a few specific GEET values. In order to determine the most suitable structure, Table 3 summarizes the maximum differences of the sparse antenna characteristics obtained after applying OCGA, EOCGA and NCOCGA for each sparse structure compared to the original one at the considered frequencies. The results allow manufacturers to make informed decisions when designing such sparse antennas.

Based on the calculated data in Table 3, it can be noticed that at the main frequencies and for all structures, the smallest differences in the results are most often observed after applying NCOCGA (underlined values in Table 3). In particular, after application of NCOCGA the smallest differences are obtained at 18 GHz for VSWR, $|S_{11}|$ and $|Z|$, at 28 GHz – for $|S_{11}|$, and at 38 GHz the smallest differences for all characteristics are obtained after applying NCOCGA. After applying OCGA, the smallest difference is obtained only at 28 GHz for VSWR and $|Z|$, while after applying EOCGA, the smallest difference is obtained only for G_{max} at 18 and 28 GHz.

In addition, when comparing the results at all frequencies with each other, the smallest differences in G_{max}, $|S_{11}|$ and $|Z|$ are obtained after NCOCGA, while in VSWR – after OCGA (values highlighted in red in Table 3). This demonstrates that NCOCGA provides higher accuracy and preserves the original antenna characteristics more than OCGA and EOCGA. NCOCGA maintains a seamless WG structure without interrupting the current path, which leads to more accurate results. However, compared to OCGA and EOCGA, NCOCGA gives sparse antennas with larger mass and more time and memory requirements for further simulations. Therefore, manufacturers should carefully evaluate their requirements and capabilities before selecting the most appropriate approach among the considered ones.

In general, the OCGA, EOCGA and NCOCGA give sparse structures that provide reasonably similar results to those of the original structure at high frequencies, regardless of the frequency in the band at which the sparse structure is obtained (bold values in Table 3). For example, the $|S_{11}|$ values at

38 GHz for all structures after applying any approach have minimal differences from its value for the original structure. Moreover, generating the sparse structure at the lowest frequency or at the central one in the frequency band regardless of the used approach provides more accurate results (italic values in Table 3). For example, at 28 GHz the G_{max} obtained for S_{18} has minimal differences compared to the G_{max} value of the original structure (24.74, 19.49, 22.02 dB), and at 38 GHz the G_{max} obtained for S_{28} has the minimal differences (15.08, 19.67, 13.26 dB). The comparison results are in good agreement with the conclusions drawn in [32]. Moreover, for antennas operating in the K/Ka band, the obtained structures not only at the minimal frequency in the frequency band, but also at the central frequency can be used to create sparse antenna structures with acceptable characteristics.

TABLE 3
COMPARING HORN ANTENNAS SPARSE STRUCTURES CHARACTERISTICS WITH THOSE OF ITS ORIGINAL STRUCTURE

***f*, GHz**	**Sparse Structures**		**Maximum Difference, %**			
			G_{max}	**VSWR**	**$\|S_{11}\|$**	**$\|Z\|$**
18	S_{18}	OCGA	*32.37*	*43.17*	*76.48*	***7.05***
		EOCGA	*30.66*	*45.18*	*83.01*	***6.67***
		NCOCGA	37.11	48.61	95.35	**7.64**
	S_{28}	OCGA	34.07	57.52	136.86	**10.45**
		EOCGA	32.51	76.3	332.04	**8.97**
		NCOCGA	*32.51*	*39.22*	*64.93*	***5.74***
	S_{38}	OCGA	76.16	86.79	724.39	**40.06**
		EOCGA	77.22	86.4	576.62	36.12
		NCOCGA	75.82	98.36	540.9	40.75
28	S_{18}	OCGA	***24.74***	***12.94***	38.04	*12.5*
		EOCGA	***19.49***	***14.99***	49.24	*15.5*
		NCOCGA	***22.02***	20.04	103.39	*17.38*
	S_{28}	OCGA	30.08	28.62	*32.55*	43.46
		EOCGA	22.16	34.5	*36.46*	39.03
		NCOCGA	23.08	***15.48***	*21.35*	21.1
	S_{38}	OCGA	45.24	67.46	51.56	55.32
		EOCGA	35.28	74.77	53.91	54.79
		NCOCGA	35.04	66.89	51.36	54.38
38	S_{18}	OCGA	37.84	21.95	**19.78**	17.94
		EOCGA	38.07	20.04	**18.39**	18.86
		NCOCGA	43.36	***14.23***	***13.83***	15.65
	S_{28}	OCGA	***15.08***	***19.26***	***17.81***	*16.37*
		EOCGA	***19.67***	***19.2***	***17.76***	*16.26*
		NCOCGA	***13.26***	19.11	**17.7**	*14.82*
	S_{38}	OCGA	**29.45**	**61.52**	**40.54**	52.25
		EOCGA	**22.45**	**38.9**	**30.26**	**29.82**
		NCOCGA	**28.69**	**43.37**	**32.58**	**33.29**

IV. SPARSE ANTENNA CHARACTERISTICS AT CERTAIN GEET

Next, in order to analyze the characteristics of the obtained sparse antennas in the operating frequency range, the GEET values of 50% and 80% were chosen as an example. Fig. 10 and Fig. 11 show the sparse structures S_{18}, S_{28}, and S_{38} obtained after applying OCGA, EOCGA and NCOCGA at the same GEET values of 50% and 80%, respectively. Analyzing the obtained sparse structures, it is noticeable that a significant number of wires along the OZ axis have been removed from the narrow wall of the original WG. This consists with the conclusion made in [35] where researchers demonstrated that the surface currents through the narrow wall of the waveguide mainly flow along the OY axis direction, which also agrees well with the waveguide theory and confirms the effectiveness of OCGA and its modification. The total numbers of remaining wires after applying OCGA, EOCGA and NCOCGA for all structures at GEET=50 and 80% are summarized in Table 4 together with the improvements that can be gained from the sparse structures in terms of the reduction in mass and computational costs. The antenna characteristics obtained for each sparse structure after applying different approaches were compared with each other and with those of the original structure in the operating frequency range. These comparisons for G_{max}, VSWR, $|S_{11}|$, and $|Z|$ at 50% and 80% GEET are shown in Fig. 12 and Fig. 13, respectively.

According to the obtained data in Fig. 12, it can be noticed that at GEET=50%, the obtained results for S_{28} and S_{18} do not differ much from the results of the original structure. Meanwhile, the obtained results for S_{38} are significantly different from those of the original structure, for example, the obtained G_{max} for S_{38} is much lower than that for S_{18}, S_{28} and the original structure. In general, Fig. 13 shows that at GEET=80% the obtained results for all structures are significantly different from the original structure. In this case, it can be noted that the advantage of reducing the antenna mass, as well as reducing the memory and time required for subsequent simulations, comes at the expense of degrading its characteristics. In addition, it is necessary to consider some special cases, for example, the structure S_{18} after the applying NCOCGA with GEET=80% gives very close characteristics to those of the original WG structure, while the improvements that can be achieved by using it are also significant (2.23 times less mass, 4.97 times less memory and 11.07 times less time than the original structure).

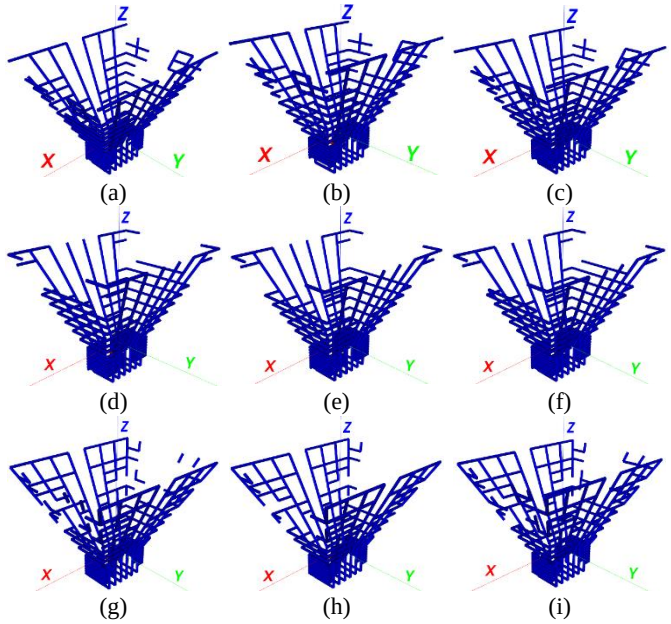

Fig. 10. Sparse horn structures after OCGA, EOCGA and NCOCGA at GEET=50%: (a, b, c) S_{18}, (d, e, f) S_{28}, (g, h, i) S_{38}

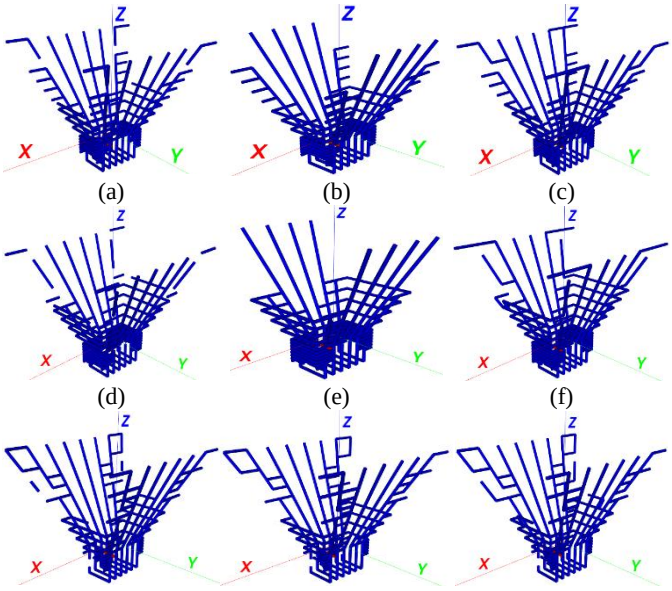

Fig. 11. Sparse horn structures after OCGA, EOCGA and NCOCGA at GEET=80%: (a, b, c) S_{18}, (d, e, f) S_{28}, (g, h, i) S_{38}

TABLE 4

TOTAL NUMBERS OF REMAINING WIRES IN THE SPARSE STRUCTURES AND THE IMPROVEMENTS RELATIVE TO THE ORIGINAL ONE

GEET, %	Sparse structures		Remaining wires	Reduction		
				Mass, times	Memory, times	Time, times
50	S_{18}	OCGA	621	1.83	3.36	6.17
		EOCGA	613	1.86	3.45	6.41
		NCOCGA	623	1.83	3.34	6.11
	S_{28}	OCGA	623	1.83	3.34	6.11
		EOCGA	623	1.83	3.34	6.11
		NCOCGA	623	1.83	3.34	6.11
	S_{38}	OCGA	613	1.86	3.45	6.41
		EOCGA	595	1.91	3.66	7.01
		NCOCGA	624	1.83	3.33	6.08
80	S_{18}	OCGA	497	2.29	5.25	12.04
		EOCGA	469	2.43	5.90	14.32
		NCOCGA	511	2.23	4.97	11.07
	S_{28}	OCGA	483	2.36	5.56	13.11
		EOCGA	463	2.46	6.05	14.89
		NCOCGA	491	2.32	5.38	12.48
	S_{38}	OCGA	413	2.76	7.61	20.98
		EOCGA	407	2.8	7.83	21.92
		NCOCGA	417	2.73	7.46	20.38

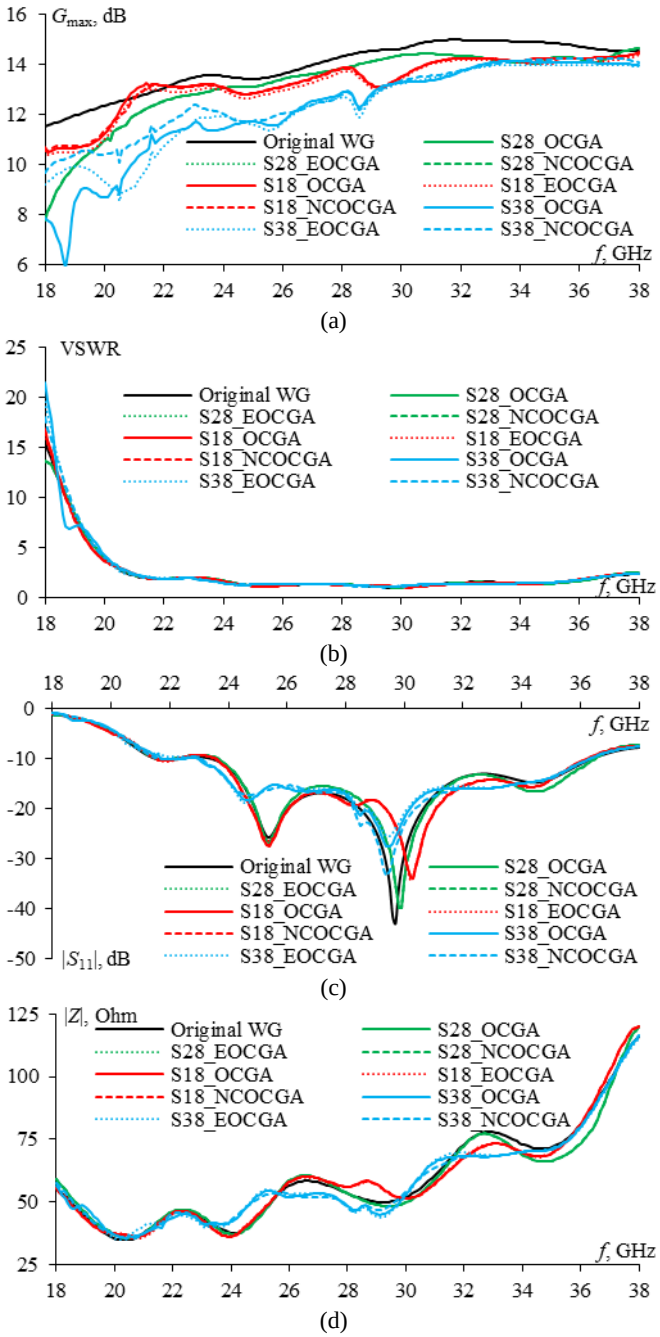

Fig. 12. Frequency dependencies of the original and sparse WG antennas after OCGA, EOCGA and NCOCGA for S_{18}, S_{28} and S_{38} at GEET=50%: (a) G_{max}, (b) VSWR, (c) $|S_{11}|$, (d) $|Z|$

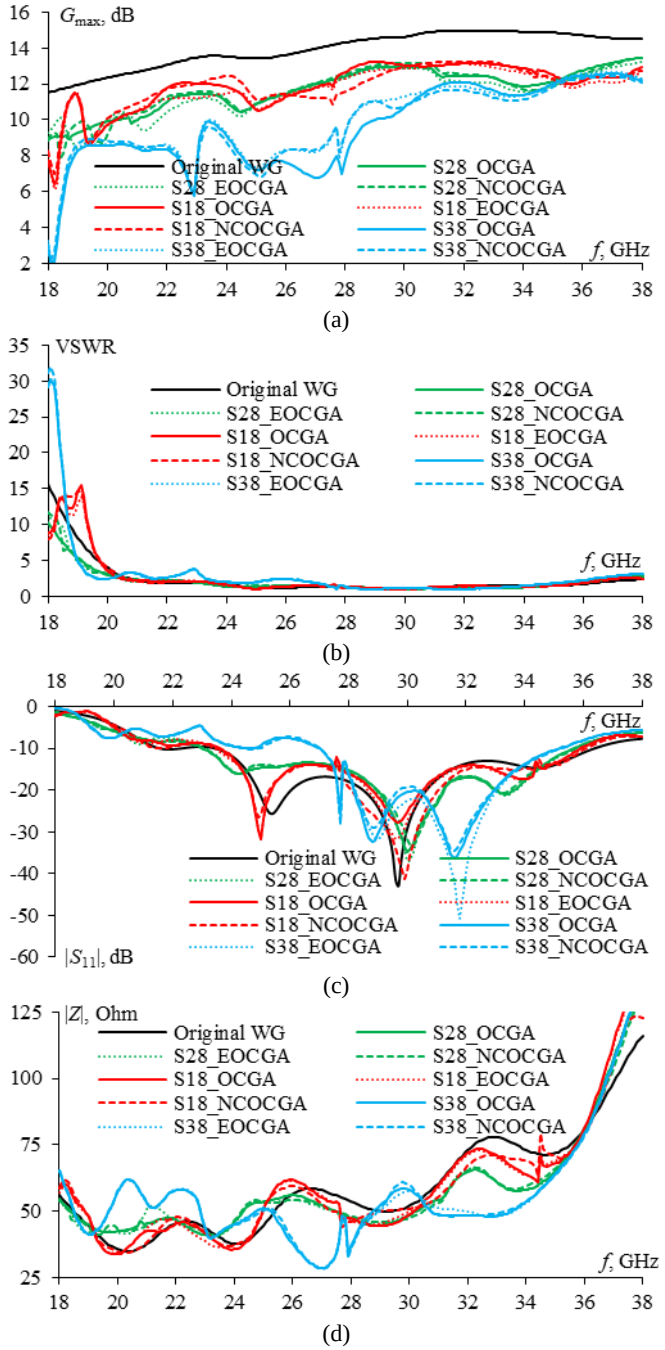

Fig. 13. Frequency dependencies of the original and sparse WG antennas after OCGA, EOCGA and NCOCGA for S_{18}, S_{28} and S_{38} at GEET=80%: (a) G_{max}, (b) VSWR, (c) $|S_{11}|$, (d) $|Z|$

V. CONCLUSION

This study investigated the influence of the choice of frequency at which the sparse structure is obtained on its resulting characteristics. The investigation considered different approaches (OCGA, EOCGA and NCOCGA) for generating the sparse structures. A comprehensive comparative analysis was performed on different sparse structures obtained at different frequencies in the K/Ka band and different GEET values. It was shown that when GEET<40%, sparse structures provide characteristics similar to those of the original structure. This demonstrates the effectiveness of the considered approaches in obtaining sparse antennas. Among these approaches, in general, NCOCGA generates sparse structures that effectively resemble the original one characteristics. However, it leads to less reduction in antenna mass and simulation time and memory requirements compared to OCGA and EOCGA.

As the GEET value increases, divergences in the obtained sparse antenna characteristics from those of the original structure become more noticeable. The study showed that in the considered frequency band the structure obtained at the minimal boundary frequency gives closer characteristics to those of the original one and more stable ones with varying the GEET value. Moreover, the structure obtained at the central frequency for this antenna also can be used since it gives acceptable results. This also was demonstrated by investigating in the operating frequency range the characteristics of sparse structures obtained at certain GEET values after applying different approaches on structures generated at different frequencies. Manufacturers can use the results of the performed analysis in this study and even perform one to choose the appropriate sparse structure that meets their specific requirements. This involves the selection of the suitable original structure and what approach to apply on it and at which GEET value.

This study is a proof of the ability of OCGA and its modifications to generate sparse antenna structures operating over a wide frequency range, such as the K/Ka band, while maintaining an acceptable level of performance. This is evidenced by the insignificant impact of these approaches on the antenna maximum gain level, as well as on preserving its impedance matching and its radiation directivity. All this despite the fact that the current distribution along the WG varies at different frequencies. Thus, the effectiveness of these approaches in designing novel sparse antennas is confirmed for X-band antennas in [32] and for K/Ka-band antennas in this paper.

In summary, this paper presents complete and detailed information on the characteristics and advantages of sparse antennas obtained after applying the optimal current grid approximation to the original structure of a horn antenna operating in the K/Ka band. This information enables the selection of a suitable sparse structure for a specific application. The study contributes to the enhancing of antenna performance and resource utilization in modern wireless communication systems.

ACKNOWLEDGEMENT

This research was funded by the Ministry of Science and Higher Education of the Russian Federation project FEWM-2023-0014.

REFERENCES

[1] N. Al-Falahy and O. Y. Alani, "Technologies for 5G Networks: Challenges and Opportunities," in *IT Professional*, vol. 19, no. 1, pp. 12-20, Jan.-Feb. 2017, DOI: 10.1109/MITP.2017.9.

[2] I. Shayea, M. Ergen, M. Hadri Azmi, S. Aldirmaz Çolak, R. Nordin and Y. I. Daradkeh, "Key Challenges, Drivers and Solutions for Mobility Management in 5G Networks: A Survey," in *IEEE Access*, vol. 8, pp. 172534-172552, 2020, DOI: 10.1109/ACCESS.2020.3023802.

[3] M. Banafaa et al., “6G Mobile Communication Technology: Requirements, Targets, Applications, Challenges, Advantages, and Opportunities,” *Alexandria Engineering Journal*, vol. 64, pp. 245–274, Feb. 2023, DOI:10.1016/j.aej.2022.08.017.

[4] N. Kishore and A. Senapati, “5G Smart Antenna for IoT Application: A Review,” *International Journal of Communication Systems*, vol. 35, no. 13, p. e5241, Sep. 2022, DOI:10.1002/dac.5241

[5] S. I. Naqvi *et al*., "An Integrated Antenna System for 4G and Millimeter-Wave 5G Future Handheld Devices," in *IEEE Access*, vol. 7, pp. 116555-116566, 2019, DOI: 10.1109/ACCESS.2019.2936513

[6] T. E. S. Oliveira, J. R. Reis, T. Fernandes, S. Madail, J. Salgado and R. F. S. Caldeirinha, "A Double Square Slot Antenna for 5G Small-Area Wireless Access Points in Street Furniture," *2023 International Wireless Communications and Mobile Computing (IWCMC)*, Marrakesh, Morocco, 2023, pp. 273-277, DOI: 10.1109/IWCMC58020.2023.10183176

[7] J. Wang, Z. Jiao, Q. Wang, Y. Zhu and K. Li, "Analysis of Novel 5G Wireless Communication Coverage Enhancing Service Mode with Power Towers and Street Lamp Poles Integrated," *2022 IEEE 6th Information Technology and Mechatronics Engineering Conference (ITOEC)*, Chongqing, China, 2022, pp. 1215-1220, DOI: 10.1109/ITOEC53115.2022.9734701

[8] C. -T. Liao, Z. -K. Yang and H. -M. Chen, "Multiple Integrated Antennas for Wearable Fifth-Generation Communication and Internet of Things Applications," in *IEEE Access*, vol. 9, pp. 120328-120346, 2021, DOI: 10.1109/ACCESS.2021.3107730

[9] R. Hussain, S. I. Alhuwaimel, A. M. Algarni, K. Aljaloud, and N. Hussain, “A Compact Sub-GHz Wide Tunable Antenna Design for IoT Applications,” Electronics, vol. 11, p. 1074, Mar. 2022, DOI:10.3390/electronics11071074

[10] T. Rashid, M. N. Hasan and P. S. Mazumdar, "An L-slot Compact Antenna for Medical, Wearable Device and IoT Applications," *2021 International Conference on Information and Communication Technology for Sustainable Development (ICICT4SD)*, Dhaka, Bangladesh, 2021, pp. 100-104, DOI: 10.1109/ICICT4SD50815.2021.9396832

[11] S. Kumar, A. S. Dixit, R. R. Malekar, H. D. Raut and L. K. Shevada, "Fifth Generation Antennas: A Comprehensive Review of Design and Performance Enhancement Techniques," in *IEEE Access*, vol. 8, pp. 163568-163593, 2020, DOI: 10.1109/ACCESS.2020.3020952

[12] S. H. Kiani, A. G. Alharbi, S. Khan, M. Marey, H. Mostafa and M. A. Khan, "Wideband Three Loop Element Antenna Array for Future 5G mmwave Devices," in *IEEE Access*, vol. 10, pp. 22472-22479, 2022, DOI: 10.1109/ACCESS.2022.3152769

[13] S. Koziel and A. Pietrenko-Dabrowska, "Reliable EM-Driven Size Reduction of Antenna Structures by Means of Adaptive Penalty Factors," in *IEEE Transactions on Antennas and Propagation*, vol. 70, no. 2, pp. 1389-1401, Feb. 2022, DOI: 10.1109/TAP.2021.3111285.

[14] A. Sidibe, A. Takacs, G. Loubet, and D. Dragomirescu, “Compact Antenna in 3D Configuration for Rectenna Wireless Power Transmission Applications,” *Sensors*, vol. 21, p. 3193, May 2021, DOI:10.3390/s21093193

[15] N. Sarker, P. Podder, M. R. H. Mondal, S. S. Shafin and J. Kamruzzaman, "Applications of Machine Learning and Deep Learning in Antenna Design, Optimization, and Selection: A Review," in *IEEE Access*, vol. 11, pp. 103890-103915, 2023, DOI: 10.1109/ACCESS.2023.3317371

[16] B. Liu *et al*., "An Efficient Method for Complex Antenna Design Based on a Self Adaptive Surrogate Model-Assisted Optimization Technique," in *IEEE Transactions on Antennas and Propagation*, vol. 69, no. 4, pp. 2302-2315, April 2021, DOI: 10.1109/TAP.2021.3051034

[17] Cavillot, C. Craeye, E. de Lera Acedo and N. Razavi-Ghods, "Efficient MoM Simulation of 3D Metallic Antenna Connected to Finite Ground Plane," *2021 IEEE International Conference on Microwaves, Antennas, Communications and Electronic Systems (COMCAS)*, Tel Aviv, Israel, 2021, pp. 193-196, DOI: 10.1109/COMCAS52219.2021.9629009

[18] T. Mao, Z. Lin, X. Zhao and W. Wu, "Electromagnetic Characteristics Analysis of Large Shipborne Array Antenna Based on Higher-Order MoM," *2020 International Conference on Microwave and Millimeter Wave Technology (ICMMT)*, Shanghai, China, 2020, pp. 1-3, DOI: 10.1109/ICMMT49418.2020.9386586

[19] B. Hamdi, D. Tihon, H. A. Kayani, F. Mesa and C. Craeye, "MoM Interaction Evaluation Intended for Antennas Printed on Ultra-Thin Substrates," *2021 15th European Conference on Antennas and Propagation (EuCAP)*, Dusseldorf, Germany, 2021, pp. 1-5, DOI: 10.23919/EuCAP51087.2021.9410951

[20] Y. -J. Zou, X. -W. Zhao, C. Guo, M. -D. Zhu and Y. Zhang, "An Integral Equation Method Using Periodic Contact-Region Modeling for Analyzing Infinitely Biperiodic Composite Structures," in *IEEE Transactions on Antennas and Propagation*, vol. 71, no. 7, pp. 6237-6242, July 2023, DOI: 10.1109/TAP.2023.3270360

[21] V. F. Martín, D. M. Solís, J. M. Taboada and F. Vipiana, "A Multiresolution Domain Decomposition Preconditioner for the MoM Solution of Multiscale Complex Structures," in *IEEE Transactions on Antennas and Propagation*, vol. 72, no. 3, pp. 2986-2991, March 2024, DOI: 10.1109/TAP.2024.3355509

[22] M. A. Colgan and M. S. Mirotznik, "Design and Fabrication of 3D Wire Grid Antenna An Integrated Method for Optimization in Constrained Volumes," *2020 IEEE International Symposium on Antennas and Propagation and North American Radio Science Meeting*, Montreal, QC, Canada, 2020, pp. 1553-1554, DOI: 10.1109/IEEECONF35879.2020.9329555

[23] Y. Zhang, B. Dong, G. Yang, D. Yang and S. Zhang, "Design Technique for a Shaped-Reflector Antenna With a Three-Layer Cable Net Structure," in *IEEE Transactions on Antennas and Propagation*, vol. 69, no. 1, pp. 109-121, Jan. 2021, DOI: 10.1109/TAP.2020.3008628

[24] A. Alhaj Hasan, A. A. Kvasnikov, D. V. Klyukin, A. A. Ivanov, A. V. Demakov, D. M. Mochalov and S. P. Kuksenko, “On Modeling Antennas Using MoM-Based Algorithms: Wire-Grid Versus Surface Triangulation,” *Algorithms*, vol. 16, no. 4, p. 200, 2023, DOI:10.3390/a16040200.

[25] A. Alhaj Hasan, M. T. Nguyen, S. P. Kuksenko and T. R. Gazizov, “Wire-Grid and Sparse MoM Antennas: Past Evolution, Present Implementation and Future Possibilities,” *Symmetry*, vol. 15(2), p. 378, 2023, DOI: 10.3390/sym15020378

[26] G. Buttazzoni, F. Babich, F. Vatta and M. Comisso, “Geometrical Synthesis of Sparse Antenna Arrays Using Compressive Sensing for 5G IoT Applications,” *Sensors*, vol. 20(2), p. 350, 2020, DOI: 10.3390/s20020350.

[27] K. Miao, Y. Zhang, S. Wang, C. Yao, G. Zhao and H. Sun, "Synthesis of Sparse Planar Antenna Arrays Using a Matrix Constraints Method," in *IEEE Transactions on Antennas and Propagation*, vol. 72, no. 5, pp. 4618-4623, May 2024, DOI: 10.1109/TAP.2024.3371642

[28] V. Yatsenko, S. A. Tretyakov, S. I. Maslovski and A. A. Sochava, "Higher order impedance boundary conditions for sparse wire grids," in *IEEE Transactions on Antennas and Propagation*, vol. 48, no. 5, pp. 720-727, May 2000, DOI: 10.1109/8.855490

[29] S. Ahn and H. Choo, "A Systematic Design Method of On-Glass Antennas Using Mesh-Grid Structures," in *IEEE*

Transactions on Vehicular Technology, vol. 59, no. 7, pp. 3286-3293, Sept. 2010, DOI: 10.1109/TVT.2010.2053227

[30] A. F. Alhaj Hasan, M. T. Nguyen, T. R. Gazizov "Modelling and Designing Wire-Grid Sparse Antennas Using MoM-based Approaches for Enhanced Performance and Reduced Cost," *Microwave Review*, vol. 29, no. 2, pp. 83–94, 2023, DOI:10.18485/mtts_mr.2023.29.2.10

[31] A. A. Hasan, T. M. Nguyen and T. R. Gazizov, "Novel MoM-Based Approaches for Generating Wire-Grid Sparse Antenna Structures," *2023 IEEE 24th International Conference of Young Professionals in Electron Devices and Materials (EDM)*, Novosibirsk, Russian Federation, 2023, pp. 570-576, DOI: 10.1109/EDM58354.2023.10225219

[32] M. T. Nguyen, A. F. Alhaj Hasan and T. R. Gazizov, "Comparative Analysis of C/OCGA Sparse Horn Antenna Structures at Different Frequencies," *2023 IEEE XVI International Scientific and Technical Conference Actual Problems of Electronic Instrument Engineering (APEIE)*, Novosibirsk, Russian Federation, 2023, pp. 530–536.

[33] D. Helena, A. Ramos, T. Varum and J.N. Matos, "The Use of 3D Printing Technology for Manufacturing Metal Antennas in the 5G/IoT Context," Sensors, vol. 21, no. 10, p. 3321, 2021, DOI:10.3390/s21103321

[34] M. T. Nguyen, A. F. A. Hasan and T. R. Gazizov, "Sparse Structures of 3D Printed K/Ka-band Horn Antenna using OCGA and its Modifications," *2024 IEEE 25th International Conference of Young Professionals in Electron Devices and Materials (EDM)*, Altai, Russian Federation, 2024, pp. 600-609, DOI: 10.1109/EDM61683.2024.10615100

[35] G. -L. Huang, S. -G. Zhou, C. -Y. -D. Sim, T. -H. Chio and T. Yuan, "Lightweight Perforated Waveguide Structure Realized by 3-D Printing for RF Applications," in *IEEE Transactions on Antennas and Propagation*, vol. 65, no. 8, pp. 3897-3904, Aug. 2017, DOI: 10.1109/TAP.2017.2715360